

## Structural Studies of the Hydrazine and Ammine Complexes of the Dinuclear Ruthenium Polysulfide Complexes

Takashi Furuhashi, Masaki Kawano, Yoshihiro Koide, Ryosuke Somazawa, and Kazuko Matsumoto\*

Department of Chemistry, Advanced Research Center for Science and Engineering, Waseda University, Tokyo 169-8555, Japan

Received April 10, 1998

The dinuclear ruthenium polysulfide complex,  $[\text{Ru}^{\text{II}}_2(\mu\text{-S}_n)(\mu\text{-S}_2\text{CNMe}_2)(\text{S}_2\text{CNMe}_2)(\text{CO})_2(\text{PPh}_3)_2]$  (**1**)·0.5CH<sub>2</sub>Cl<sub>2</sub> ( $n = 5$  or  $6$ ), was reacted with N-donor ligands, hydrazine, ammonia, and pyridine. The reaction of hydrazine with 1.2 equiv of **1**·0.5CH<sub>2</sub>Cl<sub>2</sub> affords the crystallographically characterized dinuclear Ru<sup>II</sup> complex,  $\{[\text{Ru}^{\text{II}}(\text{S}_2\text{CNMe}_2)(\text{CO})(\text{PPh}_3)]_2(\mu\text{-S}_4)(\mu\text{-N}_2\text{H}_4)\}$  (**2**)·0.5CH<sub>2</sub>Cl<sub>2</sub>. The octahedrally coordinated Ru<sup>II</sup> centers are doubly bridged by N<sub>2</sub>H<sub>4</sub> and the S<sub>4</sub> chain. The S<sub>4</sub> chain is formed through a desulfurization reaction of the S<sub>n</sub> ( $n = 5$  or  $6$ ) ligand in **1**. The reaction yield was improved in the presence of one equiv of PPh<sub>3</sub>. The space group and the cell data for **2**·0.5CH<sub>2</sub>Cl<sub>2</sub> are as follows: triclinic, space group  $P\bar{1}$  (No. 2) with  $a = 20.003(3)$  Å,  $b = 14.155(2)$  Å,  $c = 10.061(2)$  Å,  $\alpha = 110.70(1)^\circ$ ,  $\beta = 90.73(1)^\circ$ ,  $\gamma = 104.23(1)^\circ$ ,  $V = 2567.4(8)$  Å<sup>3</sup>, and  $Z = 2$ . The dinuclear ruthenium pentasulfide  $[\text{Ru}^{\text{II}}_2(\mu\text{-S}_5)(\mu\text{-S}_2\text{CNMe}_2)(\text{S}_2\text{CNMe}_2)(\text{CO})_2(\text{PPh}_3)_2]$  (**1p**) and the hexasulfide  $[\text{Ru}^{\text{II}}_2(\mu\text{-S}_6)(\mu\text{-S}_2\text{CNMe}_2)(\text{S}_2\text{CNMe}_2)(\text{CO})_2(\text{PPh}_3)_2]$  (**1h**) complexes in the crystals of **1**·0.5CH<sub>2</sub>Cl<sub>2</sub> were separated by partial recrystallization in benzene. The reaction between **1h** and NH<sub>3</sub> forms the dinuclear Ru<sup>II</sup> ammine complex,  $\{[\text{Ru}^{\text{II}}(\text{S}_2\text{CNMe}_2)(\text{CO})(\text{PPh}_3)(\text{NH}_3)]_2(\mu\text{-S}_6)\}$  (**3**)·0.5CH<sub>2</sub>Cl<sub>2</sub>, in which ammonia is terminally coordinated to the metal centers. Complex **3** crystallizes as the acetonitrile solvate in monoclinic space group  $C2/c$  (No. 15) with  $a = 30.481(7)$  Å,  $b = 12.455(2)$  Å,  $c = 15.463(3)$  Å,  $\beta = 113.90(2)^\circ$ ,  $V = 5367(1)$  Å<sup>3</sup>, and  $Z = 4$ . The reaction between **1p** and excess amount of pyridine (py) yields  $\{[\text{Ru}^{\text{II}}(\text{S}_2\text{CNMe}_2)(\text{CO})(\text{PPh}_3)(\text{py})]_2(\mu\text{-S}_5)\}$  (**4**), of which structural information was obtained by <sup>31</sup>P NMR and elemental analysis due to the poor crystal quality. Upon dissolution in CH<sub>2</sub>Cl<sub>2</sub>, both **3**·0.5CH<sub>2</sub>Cl<sub>2</sub> and **4** reinstate **1h** and **1p**, respectively, indicating that both complexes undergo intrinsically the same reaction. The N<sub>2</sub>H<sub>4</sub> ligand in **2**·0.5CH<sub>2</sub>Cl<sub>2</sub> is chemically reduced and quantitatively measured 8.4 mol % of ammonia liberation.

### Introduction

Although a number of transition metal complexes having catenated polysulfide ligands ( $\text{S}_n^{2-}$ ,  $n > 3$ ) are known, most of the studies are focused on the synthesis and structure determination, and little attention is paid on their reactivity.<sup>1,2</sup> This is probably due to the complicated chemical reactions of the ligand, which generally allows so many variable coordination modes to metals. Some examples of the coordination modes include bidentate chelation by the two terminal sulfur atoms known for  $\text{S}_3^{2-}$ ,<sup>1-3</sup>  $\text{S}_4^{2-}$ ,<sup>2,4-6</sup>  $\text{S}_5^{2-}$ ,<sup>5,7</sup>  $\text{S}_6^{2-}$ ,<sup>2,8,9</sup> and  $\text{S}_9^{2-}$ .<sup>2,10</sup> Novel tridentate

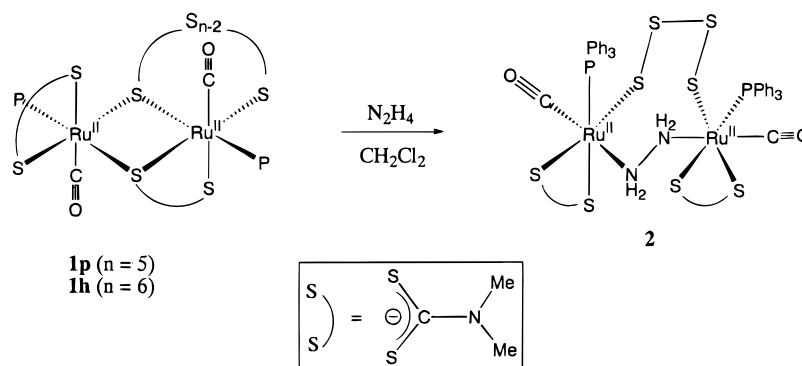
chelation is known only for  $\text{S}_7^{2-}$ .<sup>11</sup> Some polysulfides participate in both chelating and bridging two or more metals.<sup>2,12</sup> In contrast to these flourishing structural data, reported reactions of polysulfides are limited. One typical reaction of higher polysulfides (so far known up to  $\text{S}_9^{2-}$ ) is desulfurization of one or more sulfur atoms from a polysulfide chelate ring to a lower polysulfide ring, by addition of sulfur-abstracting reagents such as  $\text{PR}_3$ .<sup>1</sup> For example,  $[\text{Pt}(\text{S}_5)_3]^{2-}$  is converted to  $[\text{Pt}(\text{PPh}_3)_2(\text{S}_4)]$  and  $\text{S}^{2-}$  by addition of  $\text{PPh}_3$ .<sup>13</sup> In some reactions, addition of sulfur-abstracting reagent leads to dinucleation of a monomeric complex.<sup>14</sup> Thus, the addition of  $\text{PR}_3$  to  $\text{Cp}_2\text{TiS}_5$  gives  $(\text{Cp}_2\text{Ti})_2\text{S}_x$  ( $x = 4, 6$ ). To obtain a more general view on the reactivity, several nucleophilic and electrophilic attack to coordinated polysulfides were attempted. For example, perthiocarbonate ligand is formed by the electrophilic attack of  $\text{CS}_2$  on the coordinated  $\text{S}_4^{2-}$  ligand in  $[\text{SMo}(\text{S}_4)_2]^{2-}$ , yielding  $[\text{SMo}(\text{CS}_4)_2]^{2-}$ .<sup>15</sup> Similarly, in the reaction of  $\text{ZnS}_4(\text{PMDETA})$  ( $\text{PMDETA} = \text{N}, \text{N}', \text{N}'', \text{N}'''$ -pentamethyldiethylenetriamine) with

\* Address correspondence to this author.

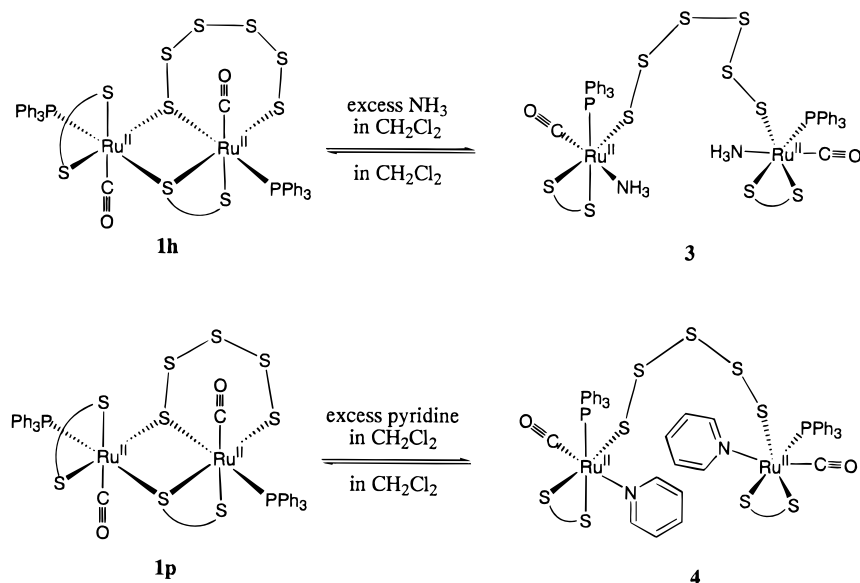
- (1) Müller, A.; Dieman, E. In *Comprehensive Coordination Chemistry*; Wilkinson, G., Gillard, R. D., McCleverty, J. A., Eds.; Pergamon: Oxford, 1987; Vol. 2, p 541.
- (2) Draganjac, M.; Rauchfuss, T. B. *Angew. Chem., Int. Ed. Engl.* **1985**, *24*, 742.
- (3) Bird, P. H.; CcCall, J. M.; Shaver, A.; Siriwardane, U. *Angew. Chem.* **1982**, *94*, 375; *Angew. Chem., Int. Ed. Engl.* **1982**, *24*, 384.
- (4) Draganjac, M.; Simhon, E.; Chan, L. T.; Kanatzidis, M.; Baenziger, N. C.; Coucouvanis, D. *Inorg. Chem.* **1982**, *21*, 3321.
- (5) Giolando, D. M.; Rauchfuss, T. B. *Organometallics* **1984**, *3*, 487.
- (6) (a) Pafford, R. J.; Rauchfuss, T. B. *Inorg. Chem.* **1998**, *37*, 1974. (b) Kim, K.-W.; Kanatzidis, M. G. *J. Am. Chem. Soc.* **1995**, *117*, 5606.
- (7) Greaney, M. A.; Coyle, C. L.; Harmer, M. A.; Jordan, A.; Stiefel, E. I. *Inorg. Chem.* **1989**, *28*, 912.
- (8) Verma, A. K.; Rauchfuss, T. B.; Wilson, S. R. *Inorg. Chem.* **1995**, *34*, 3072.
- (9) Tatsumi, K.; Inoue, Y.; Nakamura, A.; Cramer, R. E.; VanDorpe, W.; Gilje, J. W. *Angew. Chem., Int. Ed. Engl.* **1990**, *29*, 422.

- (10) (a) Marbach, G.; Strähle, J. *Angew. Chem.* **1984**, *96*, 229; *Angew. Chem., Int. Ed. Engl.* **1984**, *23*, 246.
- (11) Gotzig, J.; Rheingold, A. L.; Werner, H. *Angew. Chem., Int. Ed. Engl.* **1984**, *23*, 814.
- (12) Ramli, E.; Rauchfuss, T. B.; Stern, C. L. *J. Am. Chem. Soc.* **1990**, *112*, 4043.
- (13) Dudis, D.; Fackler, J. P., Jr. *Inorg. Chem.* **1982**, *21*, 3577.
- (14) Giolando, D. M.; Rauchfuss, T. B.; Rheingold, A. L.; Wilson, S. R. *Organometallics* **1987**, *6*, 667.
- (15) Coucouvanis, D.; Draganjac, M. *J. Am. Chem. Soc.* **1982**, *104*, 6820.

## Scheme 1



## Scheme 2



$\text{CS}_2$ , insertion of the carbon atom takes place and  $\text{ZnS}_3\text{CS}$ - $(\text{PMDETA})$  is obtained together with elemental sulfur.<sup>6a</sup> Most widely reported reaction is the addition of acetylene and its derivatives to the chelated polysulfide ligands to give dithiolene ligands,  $\text{RCSCSR}^{2-}$ .<sup>1,16</sup> For instance, the  $\text{S}_5^{2-}$  ligand in  $\text{Cp}_2\text{-TiS}_5$  reacts with  $(\text{MeCOO})\text{CC}(\text{COOMe})$  to give the dithiolene complex  $\text{Cp}_2\text{Ti}(\text{MeCOO})\text{CSCS}(\text{COOMe})$ .<sup>17</sup> Similar reaction is also reported for  $\text{Ru}(\text{bpy})_2\text{S}_5$  ( $\text{bpy} = 2,2'$ -bipyridine),<sup>7</sup> and many other polysulfide complexes.<sup>2,16</sup> Comparison of the reactivities of  $\text{ZnS}_6(\text{TMEDA})$  ( $\text{TMEDA} = \text{tetramethylethylenediamine}$ ) and  $\text{ZnS}_4(\text{PMDETA})$  toward electrophilic alkyne  $\text{C}_2(\text{CO}_2\text{Me})_2$  shows that the shorter  $\text{S}_4^{2-}$  ligand has more elevated nucleophilicity.<sup>6a,8</sup> All these reactions suggest that  $\text{S}_n^{2-}$  reacts with  $\text{RCCR}'$  to give dithiolene ligand, regardless of the sulfur number of the polysulfide ring.

Another notable reaction of polysulfide ligand is the insertion of  $\text{R}_2\text{C}$  moiety into a polysulfide chelate ring. The insertion takes place not to the metal-to-sulfur ligand bond, but to the  $\text{S-S}$  bond in the middle of the polysulfide ligand. For instance, a reaction of  $\text{Cp}_2\text{TiS}_5$  with  $\text{R}_2\text{CBr}_2$  or  $\text{R}_2\text{CO}$  ( $\text{R} = \text{H}$  or alkyl) in the presence of  $(\text{NH}_4)_2\text{S}$  produces  $1,4\text{-Cp}_2\text{TiS}_4\text{CR}_2$  and  $1,3\text{-Cp}_2\text{TiS}_4\text{CH}_2$ .<sup>5</sup> The reaction is initiated by a sulfur atom abstraction from the pentasulfide ring by  $(\text{NH}_4)_2\text{S}$  to give a bis(disulfide) complex or a mono- and trisulfide complex as the intermediate.

In contrast to the above reactions, simple polysulfide displacement reaction is known only for  $\text{ZnS}_6(\text{TMEDA})$  by

$N$ -methylimidazole.<sup>8</sup> This is not surprising, considering the general stability of  $\text{M-S}(\text{polysulfide})$  bonds. Previously, we reported the synthesis of  $\text{S}_5^{2-}$  and  $\text{S}_6^{2-}$  coordinated diruthenium(II) complexes,  $[\text{Ru}^{II}_2(\mu\text{-S}_n)(\mu\text{-S}_2\text{CNMe}_2)(\text{S}_2\text{CNMe}_2)(\text{CO})_2(\text{PPh}_3)_2]$  (**1**) ( $n = 5$  (78.5%);  $n = 6$  (21.5%)), and found that these polysulfide ligands are less electron donating than  $\text{S}^{2-}$  and  $\text{S}_2^{2-}$ , and are unstable to oxidation. In the present study, substitution reactions of **1** with  $\text{N}_2\text{H}_4$ ,  $\text{NH}_3$ , and pyridine were studied. The crystal structures of the resulting ammine complex, **2**, and the hydrazine bridged complex, **3**, were determined by X-ray crystallography, and the pyridine complex by NMR and elemental analysis. These amine complexes revert to the original polysulfide-bridged complexes **1h** and **1p**, releasing the amine ligands in the absence of excess amine ligands. These results suggest the stability of polysulfide ligands relative to amine ligands. For the hydrazine complex, reducibility of the coordinated hydrazine to  $\text{NH}_3$  was also examined.

## Results and Discussion

**Synthesis.** Previously, we reported that complex  $\text{1}\cdot 0.5\text{CH}_2\text{Cl}_2$  contains 78.5% of **1p** and 21.5% of **1h** in the lattice. The coordinates of the atoms are identical for the both complexes except the polysulfide chain length.<sup>18,19</sup> Despite this intermingling, a reaction of  $\text{1}\cdot 0.5\text{CH}_2\text{Cl}_2$  with 1.2 equiv of hydrazine provided the tetrasulfide bridged  $\text{Ru}^{II}\text{Ru}^{II}$  hydrazine complex,

(16) Coucouvanis, D. *Polyhedron* **1989**, *8*, 1716.(17) Bollinger, C. M.; Rauchfuss, T. B. *Inorg. Chem.* **1982**, *21*, 3947.(18) Uemura, H.; Kawano, M.; Watanabe, T.; Matsumoto, T.; Matsumoto, K. *Inorg. Chem.* **1992**, *31*, 5137.

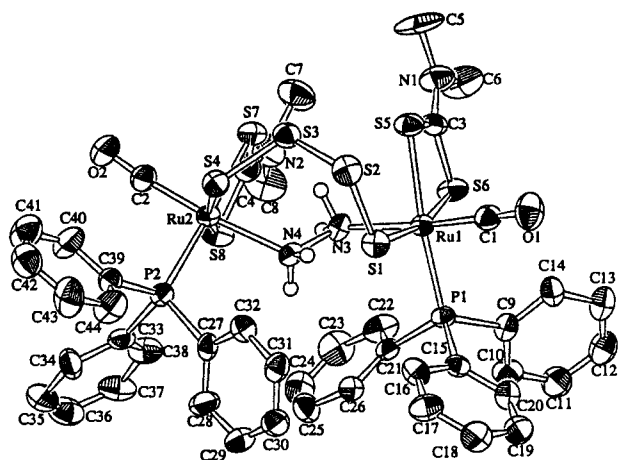


**Figure 1.** ORTEP diagram of  $\{[\text{Ru}(\text{S}_2\text{CNMe}_2)(\text{CO})(\text{PPh}_3)]_2(\mu\text{-S}_4)(\mu\text{-N}_2\text{H}_4)\} \cdot 0.5\text{CH}_2\text{Cl}_2$  showing 50% probability thermal ellipsoids for all nonhydrogen atoms.

$\{[\text{Ru}^{\text{II}}(\text{S}_2\text{CNMe}_2)(\text{CO})(\text{PPh}_3)]_2(\mu\text{-S}_4)(\mu\text{-N}_2\text{H}_4)\} \cdot 0.5\text{CH}_2\text{Cl}_2$  (Scheme 1), as a unique product.

We have successfully separated **1p** from **1h** by partial recrystallization in benzene (see Experimental Section). Complex **1h** was then reacted with large excess of  $\text{NH}_3$ . The reaction produced the dinuclear ruthenium ammine complex,  $\{[\text{Ru}^{\text{II}}(\text{S}_2\text{CNMe}_2)(\text{CO})(\text{PPh}_3)(\text{NH}_3)]_2(\mu\text{-S}_6)\} \cdot 0.5\text{CH}_2\text{Cl}_2$  (Scheme 2), with an excellent yield, and the orange X-ray quality crystals were grown by layer diffusion of ether into a  $\text{CH}_2\text{Cl}_2$  solution. The reaction of **1p** with pyridine yielded yellow crystals of  $\{[\text{Ru}^{\text{II}}(\text{S}_2\text{CNMe}_2)(\text{CO})(\text{PPh}_3)(\text{py})]_2(\mu\text{-S}_5)\} \cdot 0.5\text{CH}_2\text{Cl}_2$  (**4**) (py = pyridine). The crystals of **4** were too fragile and were not suitable for X-ray diffraction, whereas the  $^{31}\text{P}$  NMR and elemental analysis elucidated that the structure is akin to that of  $\mathbf{3} \cdot 0.5\text{CH}_2\text{Cl}_2$ . This structure was further supported by the fact that dissolution of the crystals of  $\mathbf{3} \cdot 0.5\text{CH}_2\text{Cl}_2$  and **4** in  $\text{CH}_2\text{Cl}_2$  readily reverted to **1h** and **1p**, respectively (Scheme 2).

**X-ray Crystal Structures.** Complex  $\mathbf{2} \cdot 0.5\text{CH}_2\text{Cl}_2$  crystallizes with one molecule of  $\text{CH}_2\text{Cl}_2$  in the lattice. However, refinement of the  $\text{CH}_2\text{Cl}_2$  molecule was impossible due to disorder in the position of C. Consequently, the Max Shift/Error value was limited to 4.03. The ORTEP diagram is shown in Figure 1 and the selected bond distances and angles are listed in Table 1.

The distorted octahedral coordination geometry around each ruthenium atom is completed by a bidentate dithiocarbamate, a terminal carbonyl, a triphenylphosphine, a bridging tetrasulfide, and a bridging  $\text{N}_2\text{H}_4$ . Each dithiocarbamate plane is perpendicular to the Ru–N bond. The  $\mu\text{-N}_2\text{H}_4$  group positions trans to the terminal CO groups, and separates the two Ru<sup>II</sup> centers by 5.22 Å through the zigzag Ru<sup>II</sup>NNRu<sup>II</sup> core with dihedral angle of 143.4(4)°. The observed geometry of the *trans*-Ru<sup>II</sup>-NNRu<sup>II</sup> core is similar to that in  $[\text{W}(\text{NPh})\text{Me}_3]_2(\mu\text{-}\eta^1, \eta^1\text{-NH}_2\text{-NH}_2)(\mu\text{-}\eta^2, \eta^2\text{-NHNH})$ ,<sup>20a</sup> and several other complexes,<sup>20b</sup> while we previously prepared the  $\mu\text{-N}_2\text{H}_4$  bridged Ru<sup>II</sup>Ru<sup>III</sup> mixed valence complexes, which possess the *cis*-Ru<sup>III</sup>NNRu<sup>II</sup> core.<sup>21,22</sup> The N–N distance in the bridging hydrazine (1.48(1) Å) is slightly longer than the value in analogous  $\mu\text{-N}_2\text{H}_4$ ,  $\mu\text{-S}_2$  bridged

**Table 1.** Selected Bond Distances (Å) and Angles (deg) for  $\mathbf{2} \cdot 0.5\text{CH}_2\text{Cl}_2$ <sup>a,b</sup>

Bond Distances			
Ru(1)–S(1)	2.389(3)	Ru(1)–S(5)	2.437(3)
Ru(1)–S(6)	2.414(3)	Ru(1)–P(1)	2.322(2)
Ru(1)–N(3)	2.222(8)	Ru(1)–C(1)	1.79(1)
Ru(2)–S(4)	2.407(3)	Ru(2)–S(7)	2.453(3)
Ru(2)–S(8)	2.428(3)	Ru(2)–P(2)	2.341(3)
Ru(2)–N(4)	2.228(8)	Ru(2)–C(2)	1.82(1)
S(1)–S(2)	2.058(4)	S(2)–S(3)	2.066(4)
S(3)–S(4)	2.069(4)	S(5)–C(3)	1.70(1)
S(6)–C(3)	1.726(10)	S(7)–C(4)	1.74(1)
S(8)–C(4)	1.71(1)	P(1)–C(9)	1.852(9)
P(1)–C(15)	1.833(10)	P(1)–C(21)	1.836(10)
P(2)–C(27)	1.855(10)	P(2)–C(33)	1.85(1)
P(2)–C(39)	1.851(10)	O(1)–C(1)	1.19(1)
O(2)–C(2)	1.16(1)	N(3)–N(4)	1.48(1)
Bond Angles			
S(1)–Ru(1)–S(5)	96.43(9)	S(1)–Ru(1)–S(6)	166.11(9)
S(1)–Ru(1)–P(1)	97.42(9)	S(1)–Ru(1)–N(3)	87.0(2)
S(1)–Ru(1)–C(1)	90.4(3)	S(5)–Ru(1)–S(6)	72.36(9)
S(5)–Ru(1)–P(1)	166.02(9)	S(5)–Ru(1)–N(3)	84.3(2)
S(5)–Ru(1)–C(1)	90.4(3)	S(6)–Ru(1)–P(1)	93.66(8)
S(6)–Ru(1)–N(3)	83.8(2)	S(6)–Ru(1)–C(1)	97.7(3)
P(1)–Ru(1)–N(3)	94.5(2)	P(1)–Ru(1)–C(1)	91.4(3)
N(3)–Ru(1)–C(1)	173.8(4)	S(4)–Ru(2)–S(7)	96.19(9)
S(4)–Ru(2)–S(8)	167.40(9)	S(4)–Ru(2)–P(2)	88.11(9)
S(4)–Ru(2)–N(4)	88.0(2)	S(4)–Ru(2)–C(2)	92.5(3)
S(7)–Ru(2)–S(8)	72.13(9)	S(7)–Ru(2)–P(2)	175.16(10)
S(7)–Ru(2)–N(4)	89.8(2)	S(7)–Ru(2)–C(2)	84.7(3)
S(8)–Ru(2)–P(2)	103.76(9)	S(8)–Ru(2)–N(4)	87.2(2)
S(8)–Ru(2)–C(2)	91.1(3)	P(2)–Ru(2)–N(4)	92.6(2)
P(2)–Ru(2)–C(2)	93.0(3)	N(4)–Ru(2)–C(2)	174.5(4)
Torsion Angles			
Ru(1)–S(1)–S(2)–S(3)	65.5(2)	Ru(2)–S(4)–S(3)–S(2)	–114.8(1)
Ru(1)–N(3)–N(4)–Ru(2)	143.4(4)	S(1)–S(2)–S(3)–S(4)	68.4(2)

<sup>a</sup> See Figure 1 for the atom-labeling scheme. <sup>b</sup> Numbers in parentheses are estimated standard deviations for the last significant digit.

Ru<sup>II</sup>Ru<sup>III</sup> dinuclear complex,  $\{[\text{RuCl}(\text{TMP})_2]_2(\mu\text{-Cl})(\mu\text{-N}_2\text{H}_4)(\mu\text{-S}_2)\} \cdot 0.5\text{CH}_2\text{Cl}_2$  (**5**) (TMP = trimethyl phosphite),<sup>24</sup> and is comparable to the value in free  $\text{N}_2\text{H}_4$  (1.47 Å).<sup>23</sup> The Ru–N distances (2.222(8) and 2.228(8) Å) are slightly longer than those in **5** (2.170(7) Å and 2.172(7) Å). The Ru<sup>II</sup>–S (tetrasulfide) distances (2.389(3) Å and 2.407(3) Å) are longer than the Ru<sup>II/III</sup>–S distance in **5** (2.281 Å (av)), and the Ru<sup>III</sup>–S (disulfide) distance, which usually is in the range 2.19–2.22 Å.<sup>24</sup> The observed oxidation state dependence of the Ru–S distance is a consequence of the difference in the ionic radii of Ru<sup>II</sup> and Ru<sup>III</sup>, and also in the  $\pi$ -acceptor ability of ruthenium that decreases in order of Ru<sup>III</sup> > Ru<sup>II/III</sup> > Ru<sup>II</sup>. As anticipated, the tetrasulfide chain is severely puckered (the Ru(1)–S(1)–S(2)–S(3), Ru(2)–S(4)–S(3)–S(2), and the S(1)–S(2)–S(3)–S(4) torsion angles are 65.5(2), –114.8(1), and 68.4(2)°, respectively) in order to pack in the void created by the two Ru<sup>II</sup> centers and the  $\mu\text{-N}_2\text{H}_4$  ligand. The average S–S single bond distance (2.064 Å) is a typical value found in polysulfide chains.<sup>25</sup>

Complex  $\mathbf{3} \cdot 0.5\text{CH}_2\text{Cl}_2$  also crystallizes with one molecule of  $\text{CH}_2\text{Cl}_2$  per two complex molecules in the lattice. The structure

- (19) A few examples of penta- and hexasulfide ring coexistence are reported: (a) Coucouvanis, K.; Baenziger, N. C.; Simon, E. D.; Stremple, P.; Swenson, D.; Kastikas, A.; Simopoulos, A.; Petrouleas, V.; Papaefthymiou, V. *J. Am. Chem. Soc.* **1980**, *102*, 1730. (b) Coucouvanis, D.; Patil, P. R.; Kanatzidis, M. G.; Detering, B.; Baenziger, N. C. *Inorg. Chem.* **1985**, *24*, 24.
- (20) (a) Blum, L.; Williams, I. D.; Schrock, R. R. *J. Am. Chem. Soc.* **1984**, *106*, 8316. (b) Heaton, B. T.; Jacob, C.; Page, P. *Coord. Chem. Rev.* **1996**, *154*, 193.

- (21) Kawano, M.; Hoshino, C.; Matsumoto, K. *Inorg. Chem.* **1992**, *31*, 5158.
- (22) Matsumoto, K.; Uemura, H.; Kawano, M. *Chem. Lett.* **1994**, 1215.
- (23) Cotton, F. A.; Wilkinson, G. *Advanced Inorganic Chemistry*, 5th ed.; Wiley: New York, 1988; p 316.
- (24) (a) Matsumoto, K.; Uemura, H.; Kawano, M. *Inorg. Chem.* **1995**, *34*, 658. (b) Matsumoto, K.; Matsumoto, T.; Kawano, M.; Ohnuki, H.; Shichi, Y.; Nishide, T.; Sato, T. *J. Am. Chem. Soc.* **1996**, *118*, 3597.
- (25) (a) Stuedel, R. *Angew. Chem., Int. Ed. Engl.* **1975**, *14*, 655. (b) Maheu, L. J.; Pignolet, L. H. *J. Am. Chem. Soc.* **1980**, *102*, 6348. (c) Müller, A.; Eltzner, W.; Bögge, H.; Krickemeyer, E. *Angew. Chem., Int. Ed. Engl.* **1983**, *22*, 884.



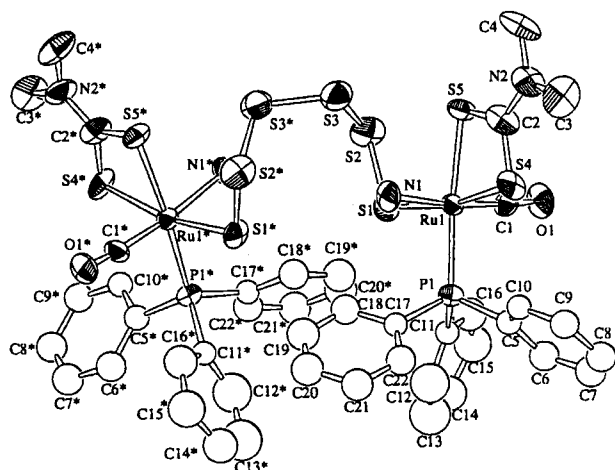


**Figure 2.** ORTEP diagram of  $\{[\text{Ru}(\text{S}_2\text{CNMe}_2)(\text{CO})(\text{PPh}_3)(\text{NH}_3)]_2(\mu\text{-S}_6)\} \cdot 0.5\text{CH}_2\text{Cl}_2$  showing 50% probability thermal ellipsoids for all nonhydrogen atoms.

is depicted in Figure 2, and the selected bond distances and angles are listed in Table 2.

Unlike  $2 \cdot 0.5\text{CH}_2\text{Cl}_2$ , however, a true crystallographic  $C_2$  axis relates the two halves of  $3 \cdot 0.5\text{CH}_2\text{Cl}_2$ . The two  $\text{Ru}^{\text{II}}$  centers are bridged by the  $\mu\text{-S}_6$  ligand, which separates the metal centers by 7.68 Å. A distorted octahedron of each  $\text{Ru}^{\text{II}}$  center is completed by a bidentate dithiocarbamate, a terminal carbonyl, a terminal ammine, and a triphenylphosphine. The  $\text{NH}_3$  group and the CO group are trans to each other that corresponds to the relation of  $\mu\text{-N}_2\text{H}_4$  to the CO group in  $2 \cdot 0.5\text{CH}_2\text{Cl}_2$ . The plane of a dithiocarbamate is perpendicular to the Ru–N bond. Unlike  $2 \cdot 0.5\text{CH}_2\text{Cl}_2$ , the polysulfide ligand remains intact throughout the reaction because, without any other bridging ligand, the  $\text{S}_6^{2-}$  chain can rearrange freely between the two  $\text{Ru}^{\text{II}}$  centers, and thus amasses no internal strain that induces desulfurization reaction. The Ru<sup>II</sup>–S (hexasulfide) distances of 2.382(5) Å is comparable to those in  $2 \cdot 0.5\text{CH}_2\text{Cl}_2$ , and thus the value is considered insensitive to presence or absence of the  $\mu\text{-N}_2\text{H}_4$  ligand.

**Reaction Mechanism.** Extended Hückel calculations of **1** show that the LUMO consists of virtually degenerate ruthenium orbitals, which will receive nucleophilic attack of the  $\text{N}_2\text{H}_4$  ligand. Upon completion of the  $\text{N}_2\text{H}_4$  coordination,  $\text{PPh}_3$  dissociation is likely to occur as a minor path, although such a product was not isolated (route A in Scheme 3).

As a major path, the other end of the  $\text{N}_2\text{H}_4$  coordinates on the other  $\text{Ru}^{\text{II}}$  atom concomitantly with cleavage of the Ru(1)–S(3) and Ru(2)–S(9) bonds (route B in Scheme 3). Significant strain is imposed on the polysulfide chain as a consequence of the four-center six-electron Ru–N–N–Ru bond formation. The free  $\text{PPh}_3$  will serve in a desulfurization reaction<sup>26</sup> that will alleviate the strain, yielding  $2 \cdot 0.5\text{CH}_2\text{Cl}_2$ . Desulfurization by  $\text{PPh}_3$  was confirmed experimentally as follows. In the course of the reaction, the reaction solution changed its color from orange to yellow, and immediate addition of excess ether resulted in precipitation of the intermediate species whose <sup>31</sup>P NMR spectrum agrees with neither  $1 \cdot 0.5\text{CH}_2\text{Cl}_2$  nor  $2 \cdot 0.5\text{CH}_2\text{Cl}_2$ . A crystallization attempt of the intermediate gave a mixture of  $1 \cdot 0.5\text{CH}_2\text{Cl}_2$  and metallic ruthenium in addition to  $\text{SPPH}_3$  in the supernatant. The desulfurization reaction of  $\text{PPh}_3$  was bolstered by the fact that the presence of 1 equiv of  $\text{PPh}_3$

**Table 2.** Selected Bond Distances (Å) and Angles (deg) for  $3 \cdot 0.5\text{CH}_2\text{Cl}_2$ <sup>a</sup>

Bond Distances			
Ru(1)–S(1)	2.382(5)	Ru(1)–S(4)	2.435(6)
Ru(1)–S(5)	2.439(6)	Ru(1)–P(1)	2.314(6)
Ru(1)–N(1)	2.21(2)	Ru(1)–C(1)	1.81(2)
S(4)–C(2)	1.72(3)	S(5)–C(2)	1.74(3)
S(1)–S(2)	2.043(9)	S(2)–S(3)	2.05(1)
P(1)–C(5)	1.84(2)	P(1)–C(11)	1.82(2)
P(1)–C(17)	1.83(2)		
Bond Angles			
S(1)–Ru(1)–S(4)	168.0(2)	S(1)–Ru(1)–S(5)	97.8(2)
S(1)–Ru(1)–P(1)	90.5(2)	S(1)–Ru(1)–N(1)	87.0(5)
S(1)–Ru(1)–C(1)	94.3(7)	S(4)–Ru(1)–S(5)	72.2(2)
S(4)–Ru(1)–P(1)	99.4(2)	S(4)–Ru(1)–N(1)	85.8(5)
S(4)–Ru(1)–C(1)	92.0(7)	S(5)–Ru(1)–P(1)	171.5(2)
S(5)–Ru(1)–N(1)	85.9(5)	S(5)–Ru(1)–C(1)	88.1(7)
P(1)–Ru(1)–N(1)	92.8(5)	P(1)–Ru(1)–C(1)	93.1(7)
N(1)–Ru(1)–C(1)	174.0(8)		

<sup>a</sup> See Figure 2 for the atom-labeling scheme.

improved yield from 39% to ca. 70%. It is not clear, however, if both **1p** and **1h** have been converted to  $2 \cdot 0.5\text{CH}_2\text{Cl}_2$  or **1p** has reacted exclusively with  $\text{N}_2\text{H}_4$ .

Resemblance of the coordination geometry of  $3 \cdot 0.5\text{CH}_2\text{Cl}_2$  with that of  $2 \cdot 0.5\text{CH}_2\text{Cl}_2$  implies that the reaction between **1h** and  $\text{NH}_3$  proceeds analogously.

**An Attempted Reduction of the Bridging  $\text{N}_2\text{H}_4$  to Ammonia.** We attempted to reduce the  $\text{N}_2\text{H}_4$  ligand in  $2 \cdot 0.5\text{CH}_2\text{Cl}_2$  to  $\text{NH}_3$  in  $\text{CH}_2\text{Cl}_2$  according to a literature method using 8 equiv of sodium amalgam as a reductant and 4 equiv of 2,6-lutidine hydrochloride as a proton source.<sup>27</sup> Liberated ammonia was trapped as  $\text{NH}_4\text{Cl}$ , which was subjected to quantitative measurement by the indophenol method.<sup>28</sup> The detected amount was only 8.4 mol % of  $\text{NH}_4^+$ , implying intrinsic difficulty in reduction of the coordinated  $\text{N}_2\text{H}_4$ . Reliability of the test was confirmed by applying the procedure to a  $\text{CH}_2\text{Cl}_2$  solution of  $3 \cdot 0.5\text{CH}_2\text{Cl}_2$ , which possesses  $\text{NH}_3$  as a ligand, to detect nearly stoichiometric amount of  $\text{NH}_4^+$  (97 mol %).

## Conclusion

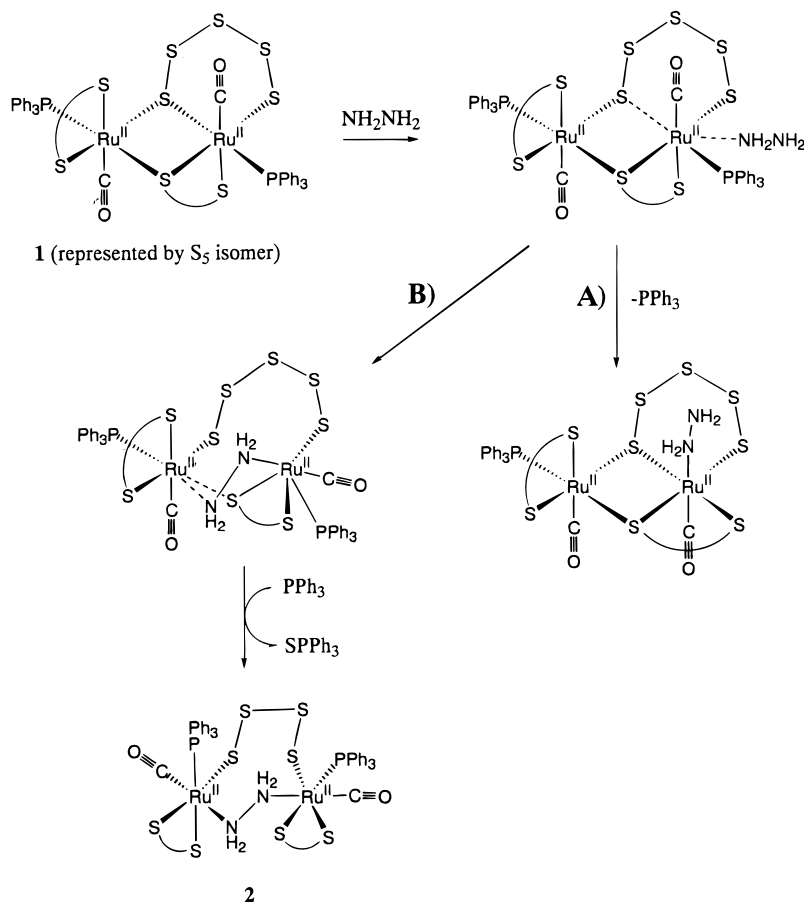
We discussed reactions of the dinuclear ruthenium polysulfides with the N-donor ligands. Hydrazine links the two  $\text{Ru}^{\text{II}}$  centers and forms the  $\text{RuNNRu}$  core that restricts relative positions of the two  $\text{Ru}^{\text{II}}$  centers in  $2 \cdot 0.5\text{CH}_2\text{Cl}_2$ . In the course of  $2 \cdot 0.5\text{CH}_2\text{Cl}_2$  formation, the polysulfide chain in **1** is converted from penta- to tetrasulfide, which then fits between the two  $\text{Ru}^{\text{II}}$  centers. On the contrary, no desulfurization reaction occurs in preparations of  $3 \cdot 0.5\text{CH}_2\text{Cl}_2$  and **4**, where the polysulfide is the only bridging ligand. The reactions in Scheme 2 are significant in that these are the second example that polysulfide undergoes substitution by amine ligand. Since the polysulfides participate both in chelating and bridging in **1h** and **1p**, the coordination of these polysulfides to the Ru atoms would be weaker than they would be if they are only chelating to the Ru atom. Nevertheless, these substitution reactions are noteworthy and give information about the relative coordination stability between polysulfide and amine ligands. Since **3** and **4** revert to **1h** and **1p**, respectively, in the absence of excess amine, these two ligands seem to have comparable coordination stability. It

(26) (a) Bolinger C. M.; Hoots, J. E.; Rauchfuss, T. B. *Organometallics* **1982**, *1*, 223. (b) Bolinger, C. M.; Rauchfuss, T. B.; Wilson, S. R. *J. Am. Chem. Soc.* **1981**, *103*, 5620.

(27) (a) Vale, M. G.; Schrock, R. R. *Inorg. Chem.* **1993**, *32*, 2767. (b) Vale, M. G.; Schrock, R. R. *Organometallics* **1993**, *12*, 1140.

(28) (a) *Japanese Industrial Standard: Testing Method for Corrosivity of Industrial Water*; JIS K 0101 36.2; Japanese Standards Association: Tokyo, Japan. (b) Chaney, A. L.; Marbach, E. P. *Clin. Chem.* **1962**, *8*, 130.

## Scheme 3



is rather surprising that amine ligands, which are usually stable, can be removed so easily in these reactions, and this suggests strong chelating tendency of the polysulfides as well as strong bridging tendency of the dithiocarbamate ligand.

Although chemical reduction of the  $\mu-N_2H_4$  to  $NH_4^+$  was not efficient enough for any practical use, electrochemical reduction of the dinuclear ruthenium complexes are planned as an alternative method and will be reported in future.

## Experimental Section

**General Methods.** All synthetic procedures were performed under purified nitrogen using standard Schlenk techniques or in a nitrogen atmosphere glovebox unless otherwise mentioned. Solvents were distilled and degassed prior to use. Solution NMR spectra were obtained on a JEOL EX-270WB spectrometer using  $CD_2Cl_2$ .  $^{31}P$  NMR chemical shifts were recorded in reference to  $P(OMe)_3/(CD_3)_2CO$  external standard (140 ppm). UV-vis spectra were recorded on a Shimadzu UV-3101PC using a quartz cuvette with 1.0 cm optical path.  $[Ru^{II}_2(\mu-S_n)(\mu-S_2CNMe_2)(S_2CNMe_2)(CO)_2(PPh_3)_2]$  (**1**) $\cdot 0.5CH_2Cl_2$  (Figure 3) was prepared as previously reported.<sup>2</sup> Molecular orbital calculations were performed within the extended Hückel formalism with use of the weighted  $H_{ij}$  formula using CaChe system.

**Crystallographic Studies.** Crystals were covered with epoxy-resin and adhered to a glass tip and mounted on a goniometer of a Rigaku AFC-7R four-circle automated diffractometer using graphite-monochromated Mo  $K\alpha$  radiation (0.710 69 Å). Data collection and cell determinations were performed in a manner previously described by using the  $\theta-2\theta$  scan technique.<sup>18</sup> Absorption correction was made based on azimuthal scans of several reflections. The data were corrected for Lorentz and polarization effects. Pertinent details are given in Table 1. The structures were solved by a direct method and the model was refined using full-matrix least-squares techniques. One molecule of  $CH_2Cl_2$  was found per complex molecule in the crystal lattice of **2** $\cdot 0.5CH_2Cl_2$ .

$Cl_2$  and **3** $\cdot 0.5CH_2Cl_2$ . All non-hydrogen atoms were refined anisotropically, except the low-occupancy chlorine atoms and the phenyl carbons in **3** $\cdot 0.5CH_2Cl_2$ , which were refined isotropically. Relevant crystallographic information is summarized in Table 3.

**Chemical Reduction of 2** $\cdot 0.5CH_2Cl_2$ . A reductant was prepared by adding 8 equiv of 2,6-lutidine hydrochloride and 4 equiv of sodium amalgam in an appropriate flask under argon atmosphere. To this flask, a  $CH_2Cl_2$  solution (10 mL) of the ruthenium complex (30 mg) was added via syringe and stirred at 0 °C. After 24 h, the solvent and volatiles were removed under vacuum. The residue was dissolved in water (50 mL) and stirred for 2 h before filtration. The filtrate was brought up to 100 mL with distilled water, and a portion (10 mL) was used for quantitative detection by the indophenol method.<sup>28</sup> First, a sodium phenoxide aqueous solution was prepared by dissolving phenol (25 g, 0.27 mol) in 55 mL of a NaOH/ $H_2O$  (20 wt %), and brought up to 200 mL with distilled water. A 0.2% EDTA/ $H_2O$  (5 mL) and a sodium phenoxide/ $H_2O$  (10 mL) were added to the filtrate under vigorous agitation. Following addition of a NaClO aqueous solution (5 mL, 1% effective Cl concentration), the solution mixture was brought up to 50 mL with distilled water, and allowed to stand at 25 °C for 40

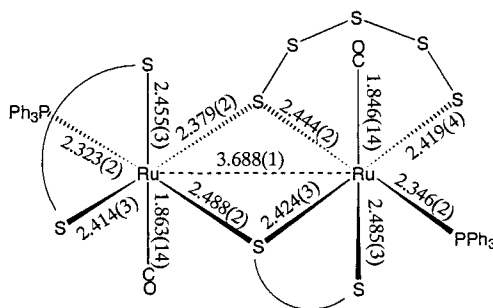


**Figure 3.** Bond distances (Å) in the diruthenium core of **1** $\cdot 0.5CH_2Cl_2$  (represented by the  $S_5$  isomer).

**Table 3.** Crystal Data for **2**·0.5CH<sub>2</sub>Cl<sub>2</sub> and **3**·0.5CH<sub>2</sub>Cl<sub>2</sub>

	<b>2</b> ·0.5CH <sub>2</sub> Cl <sub>2</sub>	<b>3</b> ·0.5CH <sub>2</sub> Cl <sub>2</sub>
formula	C <sub>44.5</sub> H <sub>47</sub> O <sub>2</sub> N <sub>4</sub> Ru <sub>2</sub> S <sub>8</sub> P <sub>2</sub> Cl	C <sub>44.5</sub> H <sub>49</sub> O <sub>2</sub> N <sub>4</sub> Ru <sub>2</sub> S <sub>10</sub> P <sub>2</sub> Cl
fw	1225.91	1292.04
cryst syst	triclinic	monoclinic
space group	<i>P</i> 1̄ (No. 2)	<i>C</i> 2/ <i>c</i> (No. 15)
<i>a</i> , Å	20.003(3)	30.481(7)
<i>b</i> , Å	14.155(2)	12.455(2)
<i>c</i> , Å	10.061(2)	15.463(3)
$\alpha$ , deg	110.70(1)	90
$\beta$ , deg	90.73(1)	113.90(2)
$\gamma$ , deg	104.23(1)	90
<i>V</i> , Å <sup>3</sup>	2567.4(8)	5367(1)
<i>Z</i>	2	4
<i>d</i> <sub>calcd</sub> , g cm <sup>-3</sup>	1.586	1.599
abs coeff ( $\mu$ ), cm <sup>-1</sup>	10.69	11.02
radiation ( $\lambda$ ), Å	Mo K $\alpha$ 0.710 69	Mo K $\alpha$ 0.710 69
<i>R</i> <sup>a</sup>	0.055	0.072
<i>R</i> <sub>w</sub> <sup>b</sup>	0.075	0.097
GOF <sup>c</sup>	1.14	1.13
<i>T</i> (deg)	20.0	20.0

<sup>a</sup>  $R = \Sigma(|F_o| - |F_c|)/\Sigma|F_o|$ . <sup>b</sup>  $R_w = [\Sigma w(|F_o| - |F_c|)^2/\Sigma w|F_o|^2]^{1/2}$ ,  $w = 1/\sigma(F_o)^2$ . <sup>c</sup> GOF =  $[\Sigma w(|F_o| - |F_c|)^2/\Sigma(N_{\text{reflens}} - N_{\text{params}})]^{1/2}$ .

min. The resulting blue solution was subjected to measure its absorbance at 630 nm. The amount of NH<sub>4</sub><sup>+</sup> was determined by using a working curve obtained by plotting the measured absorbance of standard NH<sub>4</sub>-Cl solutions as a function of the NH<sub>4</sub><sup>+</sup> concentration.

**Synthesis of {[Ru(S<sub>2</sub>CNMe<sub>2</sub>)(CO)(PPh<sub>3</sub>)<sub>2</sub>( $\mu$ -S<sub>4</sub>)( $\mu$ -N<sub>2</sub>H<sub>4</sub>)] (2)·0.5CH<sub>2</sub>Cl<sub>2</sub>.** To a CH<sub>2</sub>Cl<sub>2</sub> solution (10 mL) of [Ru<sub>2</sub>( $\mu$ -S<sub>n</sub>)( $\mu$ -S<sub>2</sub>-CNMe<sub>2</sub>)(S<sub>2</sub>CNMe<sub>2</sub>)(CO)<sub>2</sub>(PPh<sub>3</sub>)<sub>2</sub>] (**1**)·0.5CH<sub>2</sub>Cl<sub>2</sub> (50 mg, ca. 0.04 mol) was added 1.2 equiv of anhydrous hydrazine (1.6 mL) and 1.2 equiv of PPh<sub>3</sub> (13 mg) in this order at ambient temperature. The resulting orange solution was stirred for 2 h until the solution turned yellow. The solution was then allowed to stand at -40 °C for 2 days. The volume of the resulting solution was reduced to a third by evaporation prior to ether layer addition. After two weeks at 5 °C, yellow crystals of **2**·0.5CH<sub>2</sub>Cl<sub>2</sub> were obtained. Yield: 20 mg, 39%. Anal. Calcd for

C<sub>44.5</sub>ClH<sub>47</sub>N<sub>4</sub>O<sub>2</sub>P<sub>2</sub>Ru<sub>2</sub>S<sub>8</sub>: C, 43.60; H, 3.86; N, 4.57. Found: C, 43.71; H, 4.01; N, 4.27. <sup>31</sup>P NMR (ppm): 49.4.

**Separation of 1p from 1h.** The pentasulfide and the hexasulfide complexes were separated by partial recrystallization as follows. The complex **1**·0.5CH<sub>2</sub>Cl<sub>2</sub> was redissolved in the minimum amount of benzene at ambient temperature and then recrystallized at -40 °C to obtain orange crystals of **1p**. The supernatant was collected and the volume was reduced to a half by evaporation. The resulting solution was stored at -40 °C to yield crystals of **1h**.

**Synthesis of {[Ru(S<sub>2</sub>CNMe<sub>2</sub>)(CO)(PPh<sub>3</sub>)(NH<sub>3</sub>)<sub>2</sub>( $\mu$ -S<sub>6</sub>)] (3)·0.5CH<sub>2</sub>Cl<sub>2</sub>.** A CH<sub>2</sub>Cl<sub>2</sub> solution (10 mL) of [Ru<sub>2</sub>( $\mu$ -S<sub>6</sub>)( $\mu$ -S<sub>2</sub>CNMe<sub>2</sub>)(S<sub>2</sub>-CNMe<sub>2</sub>)(CO)<sub>2</sub>(PPh<sub>3</sub>)<sub>2</sub>] (50 mg, 0.04 mmol) was stirred vigorously in the presence of NH<sub>3</sub>/H<sub>2</sub>O (28%, 2 mL) for 12 h at ambient temperature. The yellow solution was layered with ether and allowed to equilibrate at 5 °C. The resulting orange crystals of **3**·0.5CH<sub>2</sub>Cl<sub>2</sub> were rinsed with ether. Yield: 49 mg, 90%. Anal. Calcd for C<sub>44.5</sub>ClH<sub>49</sub>N<sub>4</sub>O<sub>2</sub>P<sub>2</sub>Ru<sub>2</sub>S<sub>10</sub>: C, 41.37; H, 3.82; N, 4.34. Found: C, 41.50; H, 3.83; N, 4.36. <sup>31</sup>P NMR (ppm): 51.8.

**Synthesis of {[Ru( $\mu$ -S<sub>2</sub>CNMe<sub>2</sub>)(CO)(PPh<sub>3</sub>)(py)]<sub>2</sub>( $\mu$ -S<sub>5</sub>)] (4).** To a CH<sub>2</sub>Cl<sub>2</sub> solution (10 mL) of [Ru<sub>2</sub>( $\mu$ -S<sub>5</sub>)( $\mu$ -S<sub>2</sub>CNMe<sub>2</sub>)(S<sub>2</sub>CNMe<sub>2</sub>)(CO)<sub>2</sub>(PPh<sub>3</sub>)<sub>2</sub>] (**1p**) (50 mg, 0.04 mmol) was added pyridine (0.2 mL, 2.5 mmol) at ambient temperature. The solution was then stored at 5 °C to yield yellow plate-shaped crystals of **4**. Yield: 57 mg, 93%. Anal. Calcd (with a molecule of pyridine per complex molecule) for C<sub>59</sub>H<sub>57</sub>N<sub>5</sub>O<sub>2</sub>P<sub>2</sub>-Ru<sub>2</sub>S<sub>9</sub>: C, 49.88; H, 4.04; N, 4.98. Found: C, 49.58; H, 4.03; N, 5.27. <sup>31</sup>P NMR (ppm): 43.35.

**Acknowledgment.** We are grateful for the financial support of this work by CREST (Core Research for Evolutional Science and Technology) of the Japan Science and Technology Corporation (JST).

**Supporting Information Available:** X-ray crystallographic files, in CIF format, for **2**·0.5CH<sub>2</sub>Cl<sub>2</sub> and **3**·0.5CH<sub>2</sub>Cl<sub>2</sub> are available on the Internet only. Access information is given on any current masthead page.

IC9804115